Effect of Surface Recombination on Diffusion Length and Active Cavity Life time

Ali H. Khidhir

Department of Physics, College of Science, University of Baghdad, Baghdad, Iraq

Abstract

This work presents an analytical study for simulating a Fabry-Perot Bi-stable etalon (F-P cavity) filled with a dispersive optimized nonlinear optical material (Kerr type) such as semiconductors Indium Antimonite (InSb). Depending on the obtained results and because of a trade-off between the optical path length of the sample and active cavity lifetime, an optimization procedure was applied on the InSb etalon/CO laser parameters; critical switching irradiance (I_c) was applied via simulation systems of optimization procedures of optical cavity (Matlap program was used to study the optical Bi-stability of a nonlinear Fabry-Perot cavity). In order to achieve minimum switching power and faster switching time, the optimization surface recombination on the diffusion length and effective cavity lifetime was studied.

In addition, for a specific absorption value 400 cm^{-1}, the lifetime coefficient values were 0.33 , 0.091 , 0.0172 ns for sample thickness (D) = 500 , 60 , 20 μm, respectively. Also, for a bulk recombination time (T_l) of 200 ns, specific absorption (α) of 50 cm^{1}, and D of 20 μm, the surface recombination speed value was 2.845 x 10^5 cm/sec, whereas the active lifetime, which is defined as the thickness over the surface recombination speed (s_v) (D/2s_v), was equal to 3.5ns.

Keywords: Diffusion length, Fabry-perot cavity, active cavity lifetime.

<div dir="rtl">

تأثير اعادة تشكيل السطح على طول الأنتشار وعمر التجويف الفعال

علي حسن خضر

قسم الفيزياء، كلية العلوم، جامعة بغداد، بغداد، العراق

الخلاصة:

في هذا العمل ، تم اجراء دراسة تحليلية لمحاكاة مرنان فابري-بيروت (تجويف F−P)، والمملوء بمادة شبه موصلة لا خطية عالية التشتت (نوع كير) مثل انديوم-أنتيموناید (InSb). اعتماداً على ما ذكر اعلاه وبسبب التوفيق بين طول المسار البصري للنموذج داخل المرنان وعمر التجويف الفعال، تم اجراء تحسين على معلمات الليزر (Co laser) ولمرنان انديوم-أنتيموناید ، وذلك بأستخدام التبديل الشعاعي أو شدة التبديل الحرجة (Ic) عبر أنظمة محاكاة لأجراء تحسين التجويف البصري. من اجل تحقيق الحد الأدنى من قدرة التحويل وزمن تحويل سريع يجب دراسة اعادة التركيب السطحي الأمثل لطول الأنتشار وعمر التجويف الفعال.

</div>

---

*Email: alzurfialiali@gmail.com

بالأضافة الى ذلك، عندما تكون قيمة معامل الأمتصاص النوعي (α) **cm^1** 400 ستكون قيم معامل عمر

التجويف الفعال (0.0172، 0.091، 0.33) نانو ثانية وقيم سمك العينة (D) (500، 60، 20)

مايكرومتر، على التوالي.

أيضاً عندما يكون زمن اعادة التركيب الكلي (T$_l$) بحدود 200 ns، ولمعامل امتصاص نوعي (α) يساوي

50 cm^1، ولسمك عينة 20 μm، فنتيجةً لهذه القيم سنحصل على سرعة اعادة التركيب للسطح بمقدار

2.845x10^5 cm/sec، وسيكون العمر الأفتراضي الفعال والذي يعرف ب (D/2s$_v$) بقيمة 3.5 ns .

Introduction

Optical Fabry-Perot cavities are common in laser spectroscopy and interferometry and are frequently used for the stabilization of laser sources [1-2]. A novel application for high-finesse cavities was proposed in the early 1990's in the upcoming field of cavity quantum electrodynamics (cavity-QED); Single atoms are strongly coupled to a cavity-stored photon field such that the mutual coherent oscillatory exchange between both sub-systems is much faster than their individual decay rates. A number of experiments, in both the optical [3], and in the microwave regimes [4], have shown that this cavity-atom coupling can indeed be used for quantum information processing [5], where single quantum systems, such as atoms or photons, carry qubits (as the quantum alternative for the well-known bits in information science).

Since the first observation of optical Bi-stability in Indium Antimonite [6], the characterization of this system has continued. The investigation of switching dynamics of the InSb/CO system achieved progress through bandwidth measurements [7], critical slowing down [8], and noise studies [9]. These studies provided a clear understanding of the role of time constants near the bistable switch points and the limitations on switching speed.

Several parameters should be considered in order to obtain a fully optimized device, such as the beam spot size, the etalon length, the frequency of the input beam, and the absorption coefficient.

Many attempts have been made to achieve the optimum conditions of low switching power and fast switching speed of the bistable devices, using different specifications such as high finesse case [10] and low finesse case [11]. For an active F-P cavity under plane wave illumination conditions, there is a critical switching irradiance (I$_c$, as illustrated in Eq. (1)) below which bistability cannot be obtained.

Design considerations for the simplest bistable element include the selection of material, the frequency of the holding laser radiation, and hence the linear absorption and nonlinear refraction of the active medium, the sample length, and the reflectivity of the front and back sample faces. One might wish to optimize for a number of possible criteria, including minimum holding power or intensity, maximum contrast between switch-OFF and switch-ON, minimum switching speed, …. etc.

In this paper, we conduct an analytical study for simulating a Fabry-Perot bistable etalon filled with a nonlinear optical material (Kerr type), such as semiconductors (InSb) illuminated with a pulse laser. A theoretical study of a fully optimized InSb etalon (high finesse etalon) was performed. In order to achieve   the minimum switching power and faster switching time, the optimization surface recombination on the diffusion length and effective cavity lifetime was studied. In addition, for a specific absorption value of 400 cm^{-1}, the lifetime coefficient took the values of 0.33 , 0.091 , 0.0172 ns for D = 500 , 60 , 20 μm, respectively. Also, for values of T$_1$ of 200 ns, α of 50 cm^1, and D of 20 μm, the surface recombination velocity was   2.845 x 10^5 cm/sec and the effective lifetime (defined as D/2s$_v$) was 3.5ns.

Theoretical work of surface recombination effect

From the study of Frank [12], the critical switching irradiance can be estimated using:

$$I_c = \left[\frac{\lambda\alpha}{3\pi n_2}\right] f\left(R_f, R_b, \alpha D\right) \qquad \text{...................} \qquad (1)$$

where λ is the beam wavelength, α is the absorption coefficient, n_2 is the nonlinear refractive index, and R_f , R_b , αD which appear in the cavity characteristics factor represent the front face, back face reflectivity of the etalon, and the absorption length, respectively.

When the surface recombination is taken into account, equation (1) becomes:

$$I_c(\Sigma) = \frac{I_c}{S} \quad \dots\dots\dots\dots\dots\dots\dots\dots\dots\dots\dots\dots\dots\dots\dots\dots\dots,\dots\dots \quad (2)$$

where S is the surface recombination coefficient (lifetime coefficient) or:

$$I_c(\Sigma) = \frac{\lambda\alpha}{3\pi n_2} \left. f(R_f, R_b, \alpha D) \middle/ S \right. \quad \dots\dots\dots\dots\dots\dots\dots\dots\dots \quad (3)$$

and

$$S = 1 - \frac{\sum\left[\dfrac{\alpha L_D \tanh(D/2L_D)}{\tanh(\alpha D/2)} - (\alpha L_D)^2 \right]}{\left[\sum + \tanh\left(\dfrac{D}{2L_D}\right) \right]\left[1 - (\alpha L_D)^2 \right]} \quad \dots\dots\dots\dots\dots \quad (4)$$

or

$$S = 1 - \frac{\sum\left[\dfrac{\alpha L_D \left(e^{D/2L_D} - e^{-D/2L_D}\right)\left(e^{\alpha D/2} + e^{-\alpha D/2}\right)}{\left(e^{D/2L_D} + e^{-D/2L_D}\right)\left(e^{\alpha D/2} - e^{-\alpha D/2}\right)} - (\alpha L_D)^2 \right]}{\left[\sum + \dfrac{\left(e^{D/2L_D} - e^{-D/2L_D}\right)}{\left(e^{D/2L_D} + e^{-D/2L_D}\right)} \right]\left[1 - (\alpha L_D)^2 \right]} \quad \dots\dots\dots\dots \quad (5)$$

In small cavity length (less than the diffusion length), the surface recombination of the generated carriers becomes a dominant factor in comparison to the bulk recombination, due to the fact that the surface recombination becomes influential only in reducing the generated carrier concentration in the region within nearly one diffusion length of the surface [13].

Result and Discussion

The surface recombination coefficient (S) from equation (5) is plotted versus the absorption coefficient (α) as shown in Figure-1 using $L_D = 60\,\mu m$ (diffusion length) and various values of (D) (sample thickness). It can be seen from this graph that the change in the life time coefficient is very small at low absorption values (especially for $D \le L_D$) and then it becomes larger as the absorption increases. In addition, for a specific absorption value (say 400 cm^{-1}), the lifetime coefficient takes the values of 0.33, 0.091, 0.0172 for D = 500, 60, 20 μm, respectively. Figure-2 shows the dependence of S on the sample thickness for 20cm^{-1} absorption. It is clear from this figure that as the sample thickness increases, the lifetime coefficient increases and vice-versa, reaching saturation at high values of D. The effect of surface recombination on the switching time may be understood through the following cases:

(i) In small cavity length (less than the diffusion length) and low absorption value   In this case, the surface recombination coefficient becomes [14]:

$$S = \left(1 + \frac{2\sum L_D}{D} \right)^{-1} = \frac{D}{D + 2s_v T_1} \quad \dots\dots\dots\dots \quad (6)$$

where $\sum = \dfrac{s_v T_1}{L_D}$ is the surface effect, s_v is the surface recombination velocity, and T_1 is the bulk recombination time.

The result of equation (6) is plotted in Figure-3-a for T_1=200ns and α=50cm^{-1}. From this figure, using D=20μm (for example), the surface recombination velocity is 2.845×10^5 cm/sec and the effective lifetime (defined as $D/2s_v$) is equal to 3.5ns.
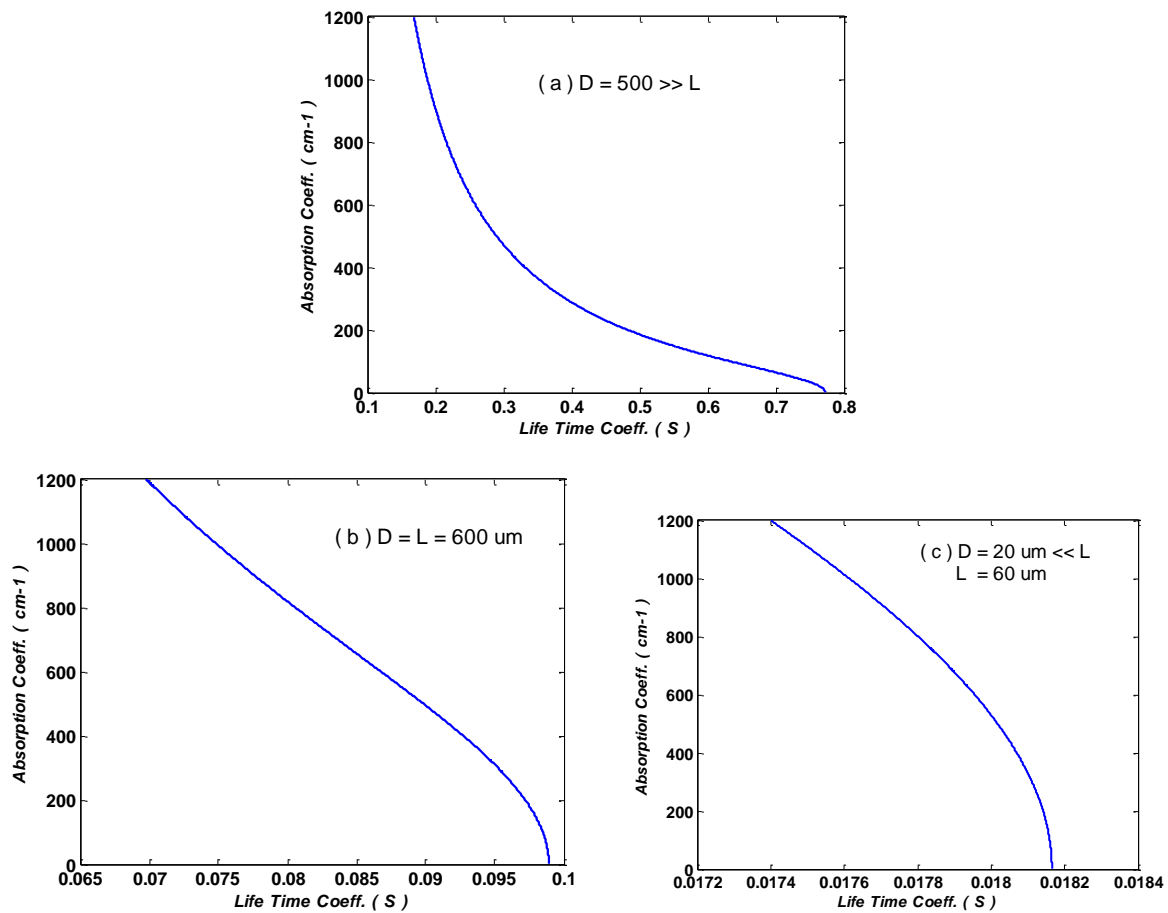
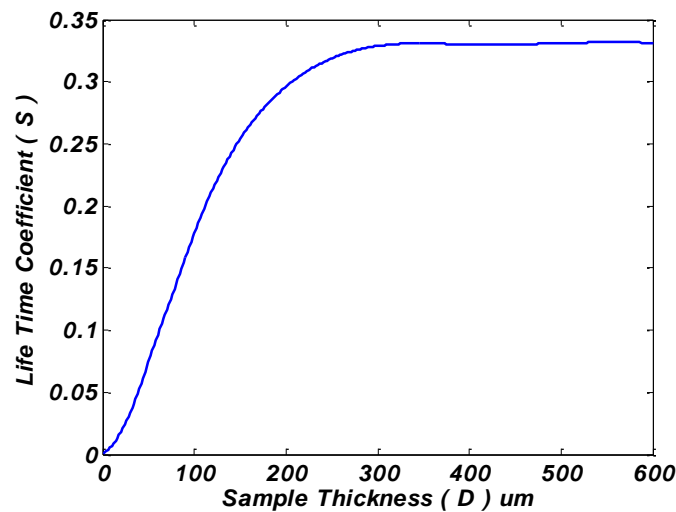**Figure 1**-Lifetime coefficient vs. absorption coefficient for different values of cavity thickness

Figure 2-Effect of the sample thickness on the surface recombination coefficient for a specific absorption $\left(\alpha = 20\,cm^{-1}\right)$
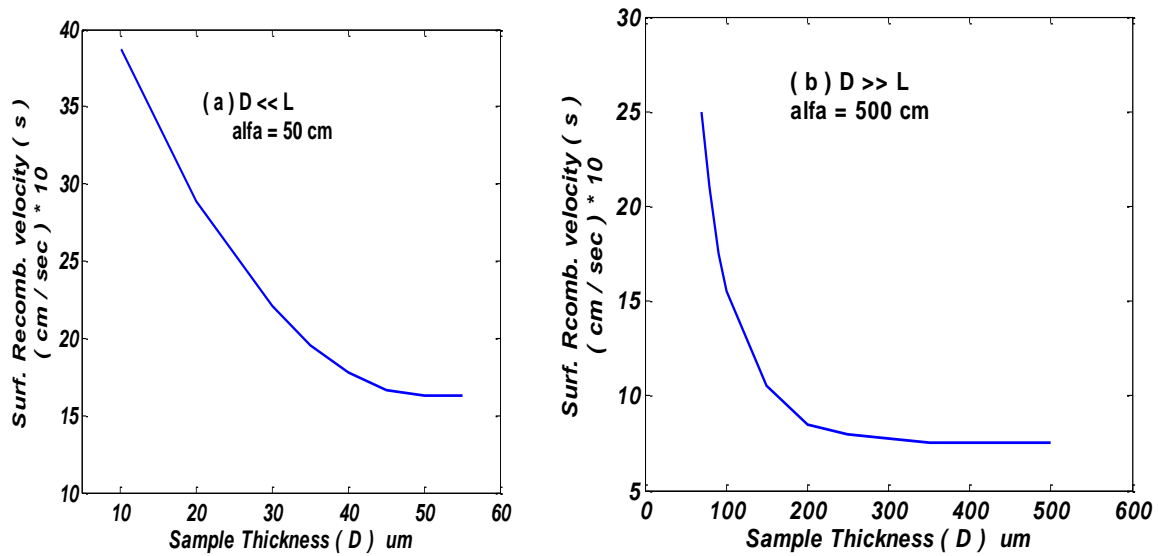
Figure 3-The dependence of surface recombination velocity on the sample thickness.
(ii) In large cavity length (more than the diffusion length) and high absorption
The surface recombination coefficient can be written as:

$$S = \frac{L_D}{L_D + s_v T_1} \qquad \text{.............................} \qquad (7)$$

Figure-(3- b) shows the results predicted from the above equation. In this case, the surface recombination velocity $\sim 7 \times 10^4 \ cm/\sec$ and the effective lifetime is about 85ns, using D=500μm and α=50cm^{-1}. It can be seen from the previous cases that the surface recombination velocity of a thin sample is much higher than that in a thick sample, due to the fact that all the carriers in a thin sample are influenced only by the surface with no bulk recombination. The effective cavity lifetime, which is defined as the product of the surface recombination coefficient with the bulk recombination time $(\tau = ST_1)$, is plotted versus the intensity for two different absorption (α=1 &10 cm^{-1}), as shown in Figure- (4 a & b). It can be seen from this figure that, for 60ns effective cavity lifetime, the required intensity with 10cm^{-1} absorption is ~300 W/cm^2, whereas it is about 30 W/cm^2 with 1cm^{-1} absorption. Thus, for a high absorption value, large incident intensity must be used in order to achieve the internal intensity necessary for switching, while for a low absorption value, or when the absorption is negligible, the optical path length of the sample is insufficient to achieve low intensity switching.
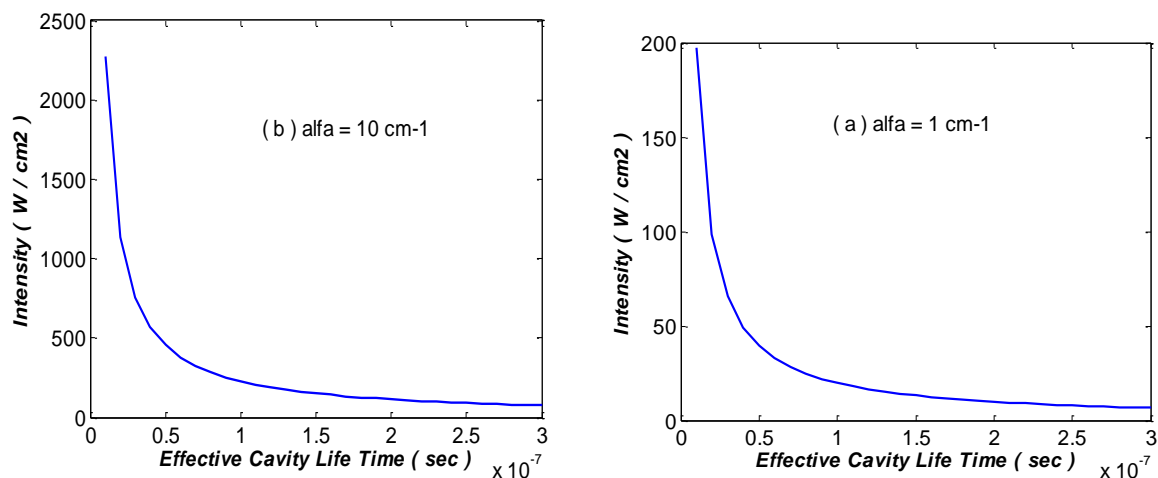

Figure 4-The intensity versus effective cavity lifetime $(\tau = ST)$ showing the strong increase in the intensity as the lifetime decreases.

Conclusions

With such natural reflectivity devices, the appropriate etalon thickness was ~150μm, and since the carrier diffusion length is ~60μm, the material time constants are dominated by the bulk recombination time of ~500ns, which in turn tends to limit the switch times. Etalon thickness of 50μm leads to a surface recombination time of ~50ns, which is the limiting time constant. From the point of interest in optical bistability in many applications, such as the demonstration of devices for digital optical computing**.**

References
1. Rafac R. J., McCall S.L.,Gibbs H.M., Churchill G.G. and Venkates T.N.C. **2017**. Sub-decahertz ultraviolet spectroscopy of 199Hg+, *Phys. Rev. Lett*. **85**: 2462.
2. Young B. C., Peyghambarian N., Gibbs H.M. and Rushford M.C. **2018**. Visible lasers with subhertz linewidths, *Phys. Rev. Lett*. **82**: 3799.
3. Turchette Q., Dagenais M. and Sharfin W.F. **2016**. Measurement of conditional phase shifts for quantum logic, *Phys. Rev. Lett*. **75**: 4710.
4. Rauschenbeutel A., Olbright G.R., Peyghambain A. F. and Macleod H.A. **2016**. Coherent operation of a tunable quantum phase gate in cavity-QED, *Phys. Rev. Lett*. **83**: 5166.
5. Bouwmeester, D. Ekert, A. and Zeilinger, A. **2000**.*The Physics of Quantum Information*, Springer,
6. Miller D.A.B., Mozolwski M.H., Miller A. and Smith S.D. **1978**. Nonlinear Optical Effects in InSb with a cw. CO Laser, *Opt. Commun*., **27**(3): 133-136.
7. Tooley F.A.P., Firth W.J., Walker A.C., MacKenzie H.A., Reid J.J. and Smith S.D., **1985**. Measurment of bandwidth of an optical transphaso, *IEEE J.Quant. Elect*., **QE-21**(9): 1356.
8. Al-Attar H.A., MacKenzie H.A. and Firth W.J., **2018**. Critical Slowing Down in an InSb optically bistable etalon, *J.Opt. Soc. Am*., **B3**: 1157.
9. MacKenzie H.A., Young J. and Iltaif A.K. **2017**. The Switching Dynamics and Noise Limitations of Indium Antimonide Bistable Element, IEEE. J. Selected Areas in Communications, **6**: 1152.
10. Miller D.A.B. **2015**. "Refractive Fabry-Perot Bistability with Linear Absorption : Theory of Operation and Cavity Optimization, *IEEE J. Quant. Electron*., **QE-17**(3): 306.
11. Wherrett B.S. **2014**. Fabry-Perot Bistable Cavity Optimization on Reflection, *IEEE J.Quant. Electron*, **QE-22**(6): 646.
12. Frank D. and Wherrett B.S. **2015**. Critical Slowing Down in an InSb optically bistable etalon, *J. Opt. Soc. Of Am*., **B4**: 25.
13. Allan G.R., MacKenzie H.A., Hunter J.J. and Wherrett B.S. **2010**. Probing a dissipative phase transition via dynamical optical hysteresis loops, *Phys. Stat. Sol*., (b) **149**: 383.
14. Goldstone J. A. and Garmire E. M. **2015**. On the dynamic response of nonlinear Fabry – Perot interferometers, *IEEE J. Quant. Electron*., **QE-17**: 366-374.